Density-based energy decomposition analysis for intermolecular interactions with variationally determined intermediate state energies

Qin Wu, Paul W. Ayers, and Yingkai Zhang

Citation: The Journal of Chemical Physics **131**, 164112 (2009); doi: 10.1063/1.3253797
View online: https://doi.org/10.1063/1.3253797
View Table of Contents: http://aip.scitation.org/toc/jcp/131/16
Published by the American Institute of Physics

Density-based energy decomposition analysis for intermolecular interactions with variationally determined intermediate state energies

Qin Wu,[1,a)] Paul W. Ayers,[2,b)] and Yingkai Zhang[3,c)]
[1]*Center for Functional Nanomaterials, Brookhaven National Laboratory, Upton, New York 11973, USA*
[2]*Department of Chemistry, McMaster University, Hamilton, Ontario L8S 4M1, Canada*
[3]*Department of Chemistry, New York University, New York 10003, USA*

(Received 14 August 2009; accepted 2 October 2009; published online 28 October 2009)

The first purely density-based energy decomposition analysis (EDA) for intermolecular binding is developed within the density functional theory. The most important feature of this scheme is to variationally determine the frozen density energy, based on a constrained search formalism and implemented with the Wu–Yang algorithm [Q. Wu and W. Yang, J. Chem. Phys. **118**, 2498 (2003)]. This variational process dispenses with the Heitler–London antisymmetrization of wave functions used in most previous methods and calculates the electrostatic and Pauli repulsion energies together without any distortion of the frozen density, an important fact that enables a clean separation of these two terms from the relaxation (i.e., polarization and charge transfer) terms. The new EDA also employs the constrained density functional theory approach [Q. Wu and T. Van Voorhis, Phys. Rev. A **72**, 24502 (2005)] to separate out charge transfer effects. Because the charge transfer energy is based on the density flow in real space, it has a small basis set dependence. Applications of this decomposition to hydrogen bonding in the water dimer and the formamide dimer show that the frozen density energy dominates the binding in these systems, consistent with the noncovalent nature of the interactions. A more detailed examination reveals how the interplay of electrostatics and the Pauli repulsion determines the distance and angular dependence of these hydrogen bonds.
 [doi:10.1063/1.3253797]

I. INTRODUCTION

Density functional theory (DFT) methods, despite their deficiency for long-range van der Waal interactions, do a reasonable job of describing intermolecular interactions. In particular, hydrogen bonds, which are responsible for a wide range of phenomena in chemistry and biology, are well described.[1–3] Like other quantum chemistry methods, DFT provides a direct access to the interaction energy at any geometry. However, when one wants to gain further insight into the interaction, it is necessary to know not only the total binding energy but also the contributions from specific types of interactions such as electrostatics, Pauli repulsion, polarization, and charge transfer. These are all physically meaningful terms, whose quantification is very useful for fine-tuning molecular interactions[4,5] and for developing molecular mechanical force field parameters.[6–8] The tool for inferring the knowledge of individual pieces in the total binding energy is generally called energy decomposition analysis (EDA), and there have been steady efforts developing such tools in quantum chemistry, using either perturbation theory[9,10] or a supermolecular approach.[11–25] However, with perhaps one exception,[26] available EDA schemes are all based on the molecular orbital (MO) theory. Since DFT is not strictly a MO theory, EDA with DFT has relied on the analogy to Hartree–Fock (HF).[27–30] It is desirable to have a density-based EDA scheme; this is the aim of this work. In addition to its theoretical appeal, we will show that there are practical advantages when the EDA is performed using densities instead of orbitals.

In the supermolecular approach, the binding energy is calculated as $\Delta E_{\text{bind}}=E_{\text{AB}}-E_{\text{A}}-E_{\text{B}}$, where A and B are the fragments and AB is the complex. The energies of A, B, and AB are all calculated variationally. An EDA introduces intermediate states to decompose the total binding energy. An early state in nearly all methods is when the fragments are brought close together but their individual identities are preserved. ΔE_{bind} can then be divided into contributions from energy changes before and after this state. Finer decompositions are achieved by dividing the former contribution into electrostatic and Pauli repulsive terms, and/or the latter into polarization and charge transfer. However, it is crucial to calculate the energy of this intermediate state, which we call the frozen density energy. Previous EDA schemes use the Heitler–London (HL) method to construct a supermolecular wave function from monomer wave functions to represent this frozen state. While this is a well-defined procedure, the HL wave function is not variationally optimized. In addition, it causes ambiguity in the separation of electrostatic and Pauli repulsion because its electron density differs from the simple addition of the fragments' densities. Thus in order to assess the electrostatic energy, the conventional EDA first uses a Hartree product of the monomer wave functions, which is not properly antisymmetrized but gives the undistorted electrostatic energy. The energy difference between

[a)]Electronic mail: qinwu@bnl.gov.
[b)]Electronic mail: ayers@mcmaster.ca.
[c)]Electronic mail: yz22@nyu.edu.

the electrostatics and the HL reference state is then termed exchange or Pauli repulsion. Unfortunately because of the density distortion, this energy includes some change in the electrostatic energy. A recent work[22] noted that it is important to use intermediate self-consistent energies that are variationally optimized while obeying the Pauli principle. While these authors provided a practical solution to this problem by separating polarization and charge transfer using their absolutely localized MOs method—a similar method based on block localized wave functions was proposed earlier for the same purpose[19]—they used the same HL approach to calculate the frozen density energy.

In this work we will present a density-based EDA that naturally applies to DFT. It respects the fact that in DFT the basic variable is the electron density and MOs are only auxiliary tools for building the density and calculating certain energy terms. In calculating the energies of intermediate states, it only uses the fragments' densities not their wave functions or density matrices. More importantly, the energy of each state is variationally optimized. A couple of recently developed methods have enabled us to achieve our goals. First, we do a constrained search to calculate the frozen density energy, implemented with the Wu–Yang (WY) algorithm.[31] Second, we use the constrained DFT method of Wu and Van Voorhis[32] to separate polarization and charge transfer. Our frozen density energy faithfully reproduces the electrostatic interactions between the fragments densities, thus we can also identify the Pauli repulsion components unambiguously. Our choice of charge transfer is based on net electron density flows in real space, which by definition is basis set independent and in practice has only a small basis set dependence. These unique features of our EDA should make it possible to gain new insights into intermolecular interactions.

In the rest of this paper we will first explain the intermediate states and the constrained methods we use to calculate their energies. We will then present our EDA results for the hydrogen bonds in the water dimer and the formamide dimer, and, finally, state our conclusions.

II. METHOD

We use some conventional terms to analyze the components of the DFT binding energy. The differences will be in the strategies to calculate these contributions. In summary, our decomposition can be written as

$$\Delta E_{\text{bind}} = \Delta E_{\text{prep}} + \Delta E_{\text{frz}} + \Delta E_{\text{pol}} + \Delta E_{\text{ct}} + \Delta E_{\text{bsse}}, \tag{1}$$

where

$$\Delta E_{\text{frz}} = \Delta E_{\text{es}} + \Delta E_{\text{Pauli}}. \tag{2}$$

The preparation energy ΔE_{prep} is a penalty paid to deform the fragments from their optimal geometries when they are isolated to their optimal geometries when they are bound. This term is necessary in a complete analysis but will not be discussed in this work since it is the same for all methods and it has been shown to be insignificant for the systems we study. Therefore we fix the internal geometries of the fragments as they are in the supermolecule, and no ΔE_{prep} is included in the reported ΔE_{bind}.

The frozen density energy ΔE_{frz} is the energy change associated with bringing the fragments from infinitely apart to their positions in the supermolecule without relaxing the fragments' electron densities. It means that the fragments' densities are simply superimposed to give the frozen density of the complex, ρ_o, and we need to calculate its energy. It is done in our scheme using the constrained search algorithm of Wu and Yang, where the Kohn–Sham system that has the same density as ρ_o is found. With such a reference system, we cannot only calculate the total energy but also identify the individual contributions from electrostatic interactions and Pauli repulsion, which include the kinetic and exchange-correlation energies.

The energy change from the frozen density to the fully relaxed density is separated into the polarization, ΔE_{pol}, and charge transfer, ΔE_{ct}, by an intermediate state where the charge of each fragment is constrained to be the same as it is in the frozen density. Thus the density is allowed to relax but there is no net flow of electrons between fragments, as defined by the real-space integration cells.

For accurate calculations of binding energies, it is important to correct the basis set superposition error (BSSE). Here we use the standard counterpoise method[33] to correct BSSE and assign the energy contribution to a separate category as ΔE_{BSSE}.

Dispersive forces, i.e., van der Waals interactions, are also an important component in intermolecular interactions. HF and most DFT methods are known to miss the dispersion; therefore it is not in our current EDA. However, we note that its contribution is relatively small to the hydrogen bonds that we study here. We will briefly discuss strategies to include van der Waals energies at the end of this paper. Below we will explain how the frozen density energy and the separation of charge transfer and polarization are done in our scheme.

A. Frozen density energy

To calculate the optimal energy for the frozen density ρ_o, we adapt a constrained minimization procedure in DFT where the total energy is minimized subject to the constraint that the density is the same as ρ_o, i.e.,

$$E[\rho_o] = \min_{\rho \to \rho_o} E[\rho]. \tag{3}$$

All energy terms that are explicit functionals of densities can be taken out of the minimization. Thus in the Kohn–Sham DFT, this minimization is equivalent to

$$E[\rho_o] = E_v[\rho_o] + E_C[\rho_o] + E_{\text{xc}}[\rho_o] + \min_{\Psi \to \rho_o} \{T_s[\Psi] + E_{\text{X}}[\Psi]\} \tag{4}$$

for a general hybrid functional. Here E_v and E_C are the electrostatic energies due to the external potential and the Coulomb interaction between electrons, E_{xc} is the pure DFT exchange-correlation energy, T_s is the kinetic energy, and E_{X} is a fraction of the HF exchange energy. Both T_s and E_{X} have

to be calculated from Ψ, a Slater determinant that is constrained to give the same density as ρ_o.

To carry out the constrained minimization, we use the direct optimization method proposed by Wu and Yang. The original WY was designed to find the lowest noninteracting kinetic energy for a given density, and it uses a Lagrangian like

$$W_s[\Psi, v(\mathbf{r})] = \sum_i^N \langle \phi_i | \hat{T} | \phi_i \rangle + \int d\mathbf{r} v(\mathbf{r}) \{\rho(\mathbf{r}) - \rho_o(\mathbf{r})\}, \quad (5)$$

where Ψ is the Slater determinant built with orbitals $\{\phi_i(\mathbf{r})\}$ and has a density $\rho(\mathbf{r}) = \Sigma_i^N |\phi_i(\mathbf{r})|^2$. Wu and Yang showed that if only the N orbitals with the lowest eigenvalues from the following equation [Eq. (6)] are used, W_s becomes a concave functional of $v(\mathbf{r})$ and the constrained search is turned into an unconstrained maximization, a much easier problem to solve,

$$[\hat{T} + v(\mathbf{r})]\phi_i = \varepsilon_i \phi_i. \quad (6)$$

Even with the HF exchange, it is straightforward to show that the proof of Wu and Yang applies to the constrained minimization in Eq. (4). Hence we can use the same algorithm. Like the original work, we will use a partial basis set expansion for $v(\mathbf{r})$, which was first developed in an efficient optimized effective potential (OEP) method.[34] The choice of $v(\mathbf{r})$ can be made for the convenience of calculations; in this work, we use the following:

$$v(\mathbf{r}) = b_{\text{ext}} v_{\text{ext}}(\mathbf{r}) + b_{\text{C}} v_{\text{C}}[\rho_o](\mathbf{r}) + f_{\text{X}} \hat{v}_{\text{X}} + \sum_t b_t g_t(\mathbf{r}). \quad (7)$$

Here v_{ext} is the external potential, $v_{\text{C}}[\rho_o]$ is the Coulomb potential due to ρ_o, $\hat{v}_{\text{X}}$ is the HF exchange potential with f_{X} being the ratio of the exact exchange in the functional used, and g_t is a set of basis functions. b_{ext}, b_{C}, and b_t are all coefficients to be optimized. There are two obvious differences in this expansion from the original work.[31] First, the nonlocal HF exchange potential is included to accommodate hybrid functionals. For a pure Kohn–Sham system, one would only use local potentials and the HF exchange would be covered as part of the basis set expansion, just as in OEP.[34] Given that there is still debate on how closely the OEP energy can approach the HF one,[35–38] we opt to use HF exchange directly, which, although not being theoretically pure Kohn–Sham will in fact introduce no computational ambiguity. At a practical level, it even reduces the burden in the expansion of the potential.

The second difference from the original WY work is that coefficients are also assigned to the external and the Coulomb potentials and will be optimized. At convergence, b_{ext} and b_{C} should of course be one. By optimizing them instead of simply setting them to one, one can take advantage of the variational conditions, i.e.,

$$\int d\mathbf{r} v_{\text{ext}}(\mathbf{r}) \{\rho(\mathbf{r}) - \rho_o(\mathbf{r})\} = 0$$

and

$$\int d\mathbf{r} v_{\text{C}}[\rho_o](\mathbf{r}) \{\rho(\mathbf{r}) - \rho_o(\mathbf{r})\} = 0,$$

ensuring that any small numerical differences between ρ and ρ_o do not affect the electrostatic energy. Their optimization only adds two more variables to the usually large set of b_t, at almost no additional cost.

We note here that there has also been great effort in studying the proper choice of basis sets to expand the potential.[39–42] For computational convenience, g_t are chosen to be atom-centered Gaussian functions like those for the orbital expansion. The balance between the basis set sizes for the orbital expansion and the potential expansion is a delicate issue, which we will not explore in this work.

B. Polarization and charge transfer

The relaxation from the frozen density to the final ground-state density of the supermolecule is realized by polarization of, and charge transfer between, the fragment densities. These two events are essentially coupled so separating them hinges on the definition of charge transfer. We define charge transfer as the net population change from the frozen density to the final density, and use the constrained DFT method of Wu and Van Voorhis[32,43] to construct an intermediate state in which the density is relaxed without charge transfer.

The constrained DFT method is a derivative of the constrained search algorithm of Wu and Yang. Instead of requiring that an electron density is matched in space, the constraint is now that a partial sum of the density, (i.e., a population), has the desired value. That is to say $\int d\mathbf{r} \rho(\mathbf{r}) w_A(\mathbf{r}) = N_A$, where N_A is the desired population number of fragment A and $w_A(\mathbf{r})$ is a weighting function that equals 1 in part of the molecule, e.g., fragment A, and 0 in the rest. For the intermediate state that we define to be fully relaxed but with no charge transfer, N_A should be exactly what one expects from the frozen density, i.e., $N_A = \int d\mathbf{r} \rho_o(\mathbf{r}) w_A(\mathbf{r})$. Thus the constraint condition we use is

$$\int d\mathbf{r} \rho(\mathbf{r}) w_A(\mathbf{r}) = \int d\mathbf{r} \rho_o(\mathbf{r}) w_A(\mathbf{r}). \quad (8)$$

We then optimize the total energy under this constraint using the method of Wu and Van Voorhis, which has been elaborated before in multiple accounts[32,43,44] and will not be repeated here. An important choice in the method is the weighting function w_A. Here we use the real-space weights based on Becke's integration scheme,[45] which has been shown before to have little basis set dependence.[46] Once the energy of this state is calculated, its difference from the frozen density energy defines ΔE_{pol}, while the difference between this energy and the final energy is ΔE_{ct}.

We note that when charge transfer is significant, the second step in this procedure can also have a substantial polarization component, as is the case in ionic bonds. A more sophisticated multistep procedure was developed by the authors for this case,[47] but it is not needed for the hydrogen bond interactions considered here.

TABLE I. The binding energy and its components for the water dimer at a geometry optimized at the MP2/aug-cc-pVQZ level (the energy unit is kJ/mol).

	HF			B3LYP			PBE		
	D	T	Q	D	T	Q	D	T	Q
ΔE_{frz}	−10.7	−9.7	−9.4	−13.6	−13.6	−13.1	−15.2	−15.4	−14.7
ΔE_{es}	−36.0	−35.3	−35.6	−34.4	−34.6	−35.0	−34.6	−34.7	−34.6
ΔE_{Pauli}	25.3	25.6	26.3	20.8	21.0	21.9	19.3	19.4	20.0
ΔE_{pol}	−3.8	−3.9	−4.2	−2.9	−2.9	−3.3	−2.8	−2.5	−3.0
ΔE_{ct}	−1.2	−1.6	−1.6	−2.6	−2.8	−2.7	−3.1	−3.3	−3.3
ΔE_{bsse}	0.8	0.3	0.2	0.7	0.4	0.2	0.7	0.5	0.2
ΔE_{bind}	−14.9	−14.9	−15.0	−18.5	−18.8	−19.0	−20.4	−20.6	−20.7

III. RESULTS

A. Water dimer

The water dimer geometry is optimized at the MP2/aug-cc-pVQZ level with Q-CHEM.[48] This structure is used for all other calculations with a development version of NWCHEM.[49]

We first examine the results at the equilibrium geometry of the dimer. Table I compares three different exchange-correlation functionals with the atomic basis sets aug-cc-pV(D, T, or Q)Z. If we look at the charge transfer energy, which is the main controversy among EDA methods, the contribution of our ΔE_{ct} to the total binding energy is 8%–10% for HF, 14%–15% for B3LYP, and 15%–16% for PBE, all smaller than previous methods. There are two reasons for this. First, our method is variational. Second, our charge transfer only considers the real-space net charge flow between fragments as compared to the frozen density, which is different from the transfer in orbital space used in wave function methods. Our ΔE_{ct} shows the trend of HF$<$B3LYP$<$PBE but the change is small. Moreover, different basis sets with the same functional give very consistent results, evident from the small percentage range given above. The insensitivity to the computational method and basis set can be attributed to the real-space fragment partitioning. Charge transfer from MO based EDA methods, on the other hand, is more sensitive because of their dependence on the highest occupied molecular orbital-lowest unoccupied orbital gap.[22]

When calculating the frozen density energy, we used the corresponding cc-pV(D, T, or Q)Z basis set, i.e., without the extra diffuse functions for the potential expansion. Our results reveal the frozen density term to be dominant and the polarization energy to be small. Within ΔE_{frz}, our ΔE_{es} is consistent with other analysis—any difference is likely due to the structure we use, which has a 2.89 Å O–O distance. Our ΔE_{Pauli} is clearly smaller than that from the HL wave function. Assuming the HL wave function captures the same Pauli repulsions, then the HL density is distorted in a way that increases the electrostatic energy from the frozen density, which would consequently end in a larger relaxation energy (i.e., polarization and charge transfer). The fact that our ΔE_{Pauli} is calculated at an undistorted frozen density thus provides a good starting point to evaluate the true relaxation energy. Because our frozen density energy is calculated variationally, it represents the best estimate of the strength of nonbonded interactions before polarization and charge transfer.

For the water dimer, we have also studied the dependence of the binding energy on the intermolecular distance. In this set of calculations, only the O···H distance that represents the hydrogen bond donor-acceptor distance is varied while all other internal coordinates are fixed to be those in the optimized structure of MP2/aug-cc-pVQZ. All calculations are done at the B3LYP/aug-cc-pVQZ level using cc-pVTZ for the potential expansion of Wu and Yang. Our results are tabulated in Table II. In Fig. 1 we also plot the frozen density, polarization, and charge transfer components, as well as the total binding energy. It is interesting to see how closely ΔE_{frz} follows ΔE_{bind}. ΔE_{frz} is solely responsible for the long-range tail because ΔE_{pol} and ΔE_{ct} decay quickly with increasing distance. ΔE_{frz} also gives an equilibrium distance that is only about 0.1 Å too long and a binding energy 4.2 kcal/mol smaller than ΔE_{bind}. These differences are compensated by the increase in ΔE_{pol} and ΔE_{ct}. ΔE_{pol} rises much more rapidly than ΔE_{ct} as the distance is shortened, but this increase is not enough to overcome the steep short-range wall setup by ΔE_{frz}.

The electrostatic and the Pauli repulsion components that make up the frozen density energy are opposite in sign but have similar magnitudes. For better comparison, we plot their absolute values in Fig. 2. It is immediately clear that there is a balance point at about 1.7 Å, beyond which the electrostatics are more important, while quantum effects (i.e., the Pauli repulsion) take over when the fragments are too close. As an attempt to explore the usefulness of our method in force field development, we fit our data to analytical potential functions. We choose to expand the electrostatic energy in terms of interactions that include dipoles only or both dipoles and quadrupoles,

$$f_{\text{es}}^{n}(R) = \sum_{i=3}^{n} -\frac{C_i}{R^i}, \quad n = 3 \text{ or } 5, \tag{9}$$

and we use the Born–Mayer form for the repulsion,

$$f_{\text{Pauli}}(R) = a \exp(-bR). \tag{10}$$

It is already known that quadrupoles are important in describing the interaction of water molecules,[50,51] and the exponential form gives a good account of the short-range repulsion.[5] Our results agree with these conclusions. The excellent fits produced by f_{es}^{5} and f_{Pauli}, as shown in Fig. 2, also suggest that our EDA indeed gives meaningful separation of electrostatics and the Pauli repulsion.

TABLE II. The binding energy and its components at selected intermolecular distances in the water dimer calculated at the B3LYP/aug-cc-pVQZ level (units are angstrom for R_{OH} and kJ/mol for energies).

	ΔE						
R_{OH}	es	Pauli	frz	pol	ct	BSSE	bind
1.4	−113.4	166.4	53.0	−21.9	−8.3	0.3	23.0
1.6	−71.1	79.0	7.9	−9.8	−5.5	0.3	−7.2
1.8	−46.0	36.8	−9.2	−4.7	−3.6	0.2	−17.3
1.9	−37.6	24.9	−12.7	−3.3	−2.9	0.2	−18.8
2.0	−31.0	16.7	−14.3	−2.4	−2.4	0.2	−18.9
2.1	−25.9	11.2	−14.7	−1.8	−1.9	0.2	−18.3
2.2	−21.9	7.4	−14.5	−1.4	−1.6	0.1	−17.2
2.4	−16.0	3.2	−12.8	−0.9	−1.0	0.1	−14.6
2.6	−12.2	1.4	−10.8	−0.6	−0.6	0.1	−12.0
3.0	−7.7	0.3	−7.4	−0.4	−0.3	0.1	−7.9
4.0	−3.2	0.2	−3.0	−0.3	0.0	0.0	−3.3
5.0	−1.6	0.1	−1.5	−0.2	0.0	0.0	−1.7
6.0	−0.9	0.1	−0.8	−0.2	0.0	0.0	−1.0
7.0	−0.5	0.1	−0.4	−0.1	0.0	0.0	−0.6
8.0	−0.3	0.0	−0.3	−0.1	0.0	0.0	−0.4

There exists a large volume of EDA studies on the water hydrogen bonds and some controversy over the importance of covalence binding. The conclusion necessarily depends on the type of EDA that is performed. Because our method is based on densities, rather than orbitals, some of the critiques of earlier interpretations no longer apply. For instance, in our method a proper antisymmetrized wave function is obtained without changing the frozen density; this permits us to totally separate the effects of antisymmetrization (Pauli principle) from the accumulation of electron density in the bonding regions (covalency). This could provide an alternative perspective on Compton profile anisotropies[27,52] in the water dimer. Charge transfer is often used an indicator of covalency. Here, different methods give very different answers. In particular, studies using the Kitaura–Morokuma analysis and its variations[13,18,53,54] predict a much smaller contribution of charge transfer than those based on natural bonding orbitals.[17,29] Our method has probably the smallest amount of charge transfer, even when compared to other variational methods.[19,22] As discussed above, this result is due to a combination of being variational and using real-space partitions. This real-space partition prevents us from quantitatively connecting the charge transfer to covalency. However, the dominance of the frozen density energy in the binding does agree with chemical intuition about the noncovalent nature of hydrogen bonds.

B. Formamide dimer

As an example of the angular dependence of the hydrogen bond energy, we study the out-of-plane formamide dimer. This dimer has long been used as a minimal model for hydrogen bonds in proteins and nucleic acids.[55–60] Several stable structures of the dimer have been identified;[61,62] the out-of-plane geometry is used mainly to compare with the single hydrogen bonds in protein side chains.[63] In this work, we focus on the hydrogen bonding energy dependence on the angle at the acceptor atom (Ψ) and keep other internal coordinates fixed at their optimal values. We use the reference definition of Ψ.[63] Figure 3 shows the structure of three Ψ

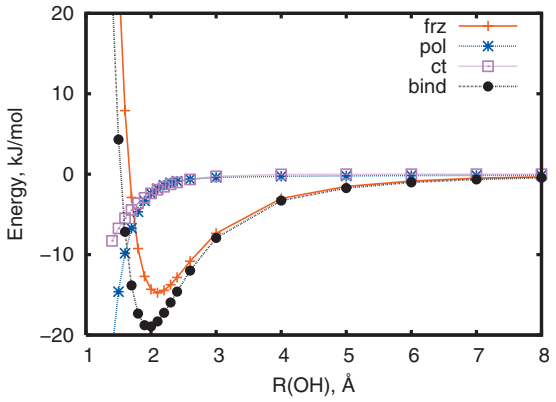

FIG. 1. The binding energy and its components at different intermolecular distances in the water dimer. Points are the results at B3LYP/aug-cc-pVQZ level. Lines are only for guiding eyes.

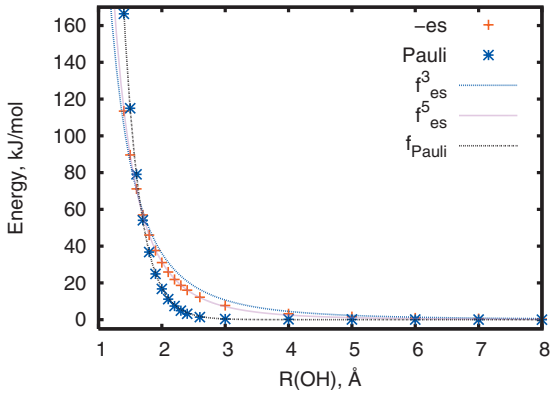

FIG. 2. The electrostatic and the Pauli components of the binding energy at different intermolecular distances in the water dimer. Points are the results at B3LYP/aug-cc-pVQZ level. Lines are their fitted functions. Note that the negative of the electrostatic energy is plotted.

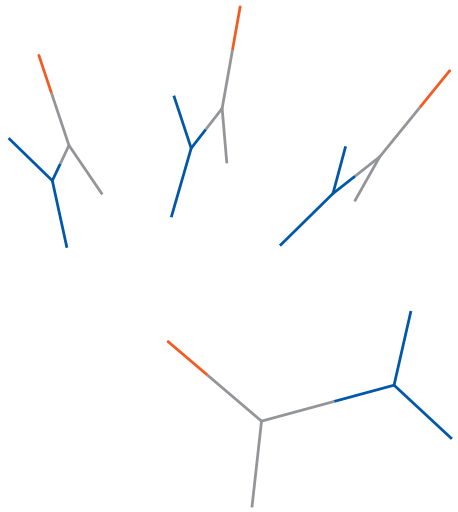

FIG. 3. The formamide dimers formed by the three hydrogen bond donor molecules at the top and the acceptor at the bottom have angles at the acceptor atom (Ψ) of 160°, 130°, and 100°, respectively, from left to right.

values. We use B3LYP and aug-cc-pVDZ basis set both for the geometry optimization and EDA. The basis set cc-pVDZ is used in the potential expansion.

It has been shown that DFT calculations present a well-defined minimum in the binding energy dependence on Ψ, in good agreement with observations in protein structures.[63] Our calculations confirm this feature, as can be seen in Fig. 4 and Table III. A closer look of the energy components reveals that the dependence is mainly determined by the frozen density energy. This is very interesting because molecular mechanical force fields have shown only limited degree of accuracy[63] and our results suggest possible ways for improvement. In particular, while the polarization and charge transfer are important to obtain the exact minimum, the electrostatics and the Pauli repulsion are essential for obtaining the correct curvature. We also plotted in Fig. 5 the latter two terms from our analysis, again using their absolute values. Comparing to ΔE_{es}, ΔE_{Pauli} is flatter at larger angles but increases more rapidly when the angle decreases. However, even at the smallest angle studied here, there is still such a significant distance between the monomers that the repulsion is not strong enough to overcome the electrostatic attraction.

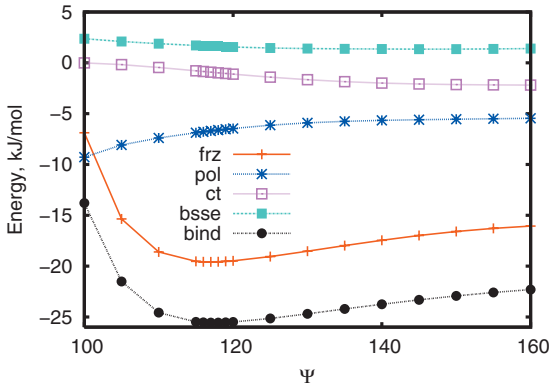

FIG. 4. The binding energy and its components at different angle of the acceptor atom in the formamide dimer. Points are the results at B3LYP/aug-cc-pVDZ level. Lines are only for guiding eyes.

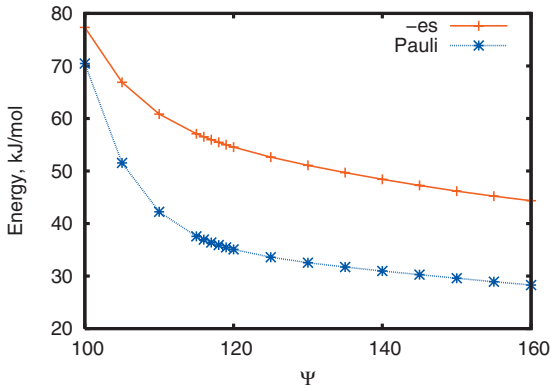

FIG. 5. The electrostatic and the Pauli components of the binding energy at different angles of the acceptor atom in the formamide dimer. Points are the results at B3LYP/aug-cc-pVDZ level. Lines are only for guiding eyes. Note that the negative of the electrostatic energy is plotted.

It is interesting that neither term has a minimum Ψ. The minimum in ΔE_{frz} is a result of balancing the two effects. Therefore, when improving the electrostatics and polarization effects in force fields to describe hydrogen bonds, one also needs to pay close attention to the repulsion.

We note again in our calculations the small contribution from charge transfer. ΔE_{ct} amounts for 10% of the total binding at the largest angle and decreases smoothly to zero contribution at the smallest angle. The polarization shows an opposite trend. It becomes the dominant factor of the total binding at the smallest angle, stronger than the frozen density energy. This is expected because the overlap between the two molecules becomes much more significant at that angle, which leads to not only larger stabilization effects from polarization but also larger Pauli repulsion.

IV. CONCLUSION

By using densities as the basic variables and the powerful tools of constrained search in DFT, we have presented in this work the first EDA method that produces variationally determined frozen density energies as well as charge transfer energies. There are several advantages of our new approach when applied to intermolecular interactions. First, the contribution of the frozen density energy to the total binding energy is truly dominant, while those of polarization and charge transfer are small. These trends are potentially helpful for force field development. Second, because the electrostatic and Pauli repulsion energies are calculated together as part of the frozen density energy, there is no more contribution from density distortion in the Pauli repulsion term; this allows for an unambiguous interpretation of the frozen density energy. Third, the phenomena of polarization and charge transfer are modeled directly as deformations of the molecular density in real space, which is applicable even in the complete basis set limit, in contrast to orbital based methods.

We have applied our method to the hydrogen bond analysis of the water dimer and the formamide dimer. Our results suggest that charge transfer only contributes about 15% to hydrogen bonding of the water dimer. As functions of the intermolecular distance, our electrostatic energies and Pauli repulsion energies are accurately fit by simple analytic

TABLE III. The binding energy (kJ/mol) and its components at some selected angles (Ψ,°) of the acceptor atom in the formamide dimer.

	ΔE						
Ψ	es	Pauli	frz	pol	ct	BSSE	bind
100	−77.3	70.5	−6.9	−9.3	−0.0	2.4	−13.8
105	−66.9	51.5	−15.4	−8.1	−0.2	2.1	−21.5
110	−60.8	42.2	−18.6	−7.4	−0.4	1.9	−24.6
116	−56.5	36.9	−19.6	−6.8	−0.8	1.7	−25.5
118	−55.5	35.9	−19.6	−6.6	−1.0	1.6	−25.6
120	−54.6	35.1	−19.5	−6.4	−1.1	1.6	−25.5
125	−52.6	33.6	−19.0	−6.1	−1.4	1.4	−25.1
130	−51.1	32.5	−18.5	−5.9	−1.7	1.4	−24.7
140	−48.4	31.0	−17.4	−5.7	−2.0	1.4	−23.8
150	−46.2	29.6	−16.6	−5.5	−2.1	1.3	−22.9
160	−44.3	28.3	−16.1	−5.4	−2.2	1.4	−22.3

forms. For the formamide dimer, electrostatics and the Pauli repulsion work together to give the correct angular dependence of the binding strength.

Our method provides the first complete purely density-based analysis of the binding energy and we have shown that the components in our analysis are all very meaningful. We are very optimistic about the usefulness of our method for the development of new molecular mechanical force fields. We are currently carrying out studies along this avenue and will present our results in future account.

A missing piece in our current analysis is the long-range dispersion term, which is not included in most DFT methods. There are empirical corrections that add dispersion to DFT,[64–66] mostly as standing-alone terms outside of the self-consistent calculations. For those methods, no new development in the decomposition is needed to obtain the dispersion term. Great progress has also been made recently in the development of van der Waals functionals.[67–70] Those functionals have a term that is designed specifically for the long-range dispersion so there is no obstacle to separating it from the total energy, although one has to decide which density to be used for its calculation. We will explore this issue in our future work. Another direction to expand the current work is for intramolecular interactions. We note that the constrained DFT method has been previously applied to covalent and ionic bonds.[44] We are working to implement a full EDA for such bonds with our density-based approach.

ACKNOWLEDGMENTS

Research carried out at the Center for Functional Nanomaterials, Brookhaven National Laboratory was supported by the U.S. Department of Energy, Office of Basic Energy Sciences, under Contract No. DE-AC02-98CH10886. Y.Z. acknowledges the support from the NSF (Grant No. CHE-CAREER-0448156). P.W.A. acknowledges the NSERC, the Sloan Foundation, and Sharcnet.

[1] F. Sim, A. St. Amant, I. Papai, and D. Salahub, J. Am. Chem. Soc. **114**, 4391 (1992).
[2] J. J. Novoa and C. Sosa, J. Phys. Chem. **99**, 15837 (1995).
[3] P. R. Rablen, J. W. Lockman, and W. L. Jorgensens, J. Phys. Chem. A **102**, 3782 (1998).
[4] A. J. Stone, *The Theory of Intermolecular Forces* (Oxford University Press, New York, 1997).
[5] A. J. Stone, Science **321**, 787 (2008).
[6] J. P. Piquemal, G. A. Cisneros, P. Reinhardt, N. Gresh, and T. A. Darden, J. Chem. Phys. **124**, 104101 (2006).
[7] N. Gresh, G. A. Cisneros, T. A. Darden, and J. P. Piquemal, J. Chem. Theory Comput. **3**, 1960 (2007).
[8] G. A. Cisneros, T. A. Darden, N. Gresh, P. Reinhardt, O. Parisel, J. Pilme, and J.-P. Piquemal, in *Multi-scale Quantum Models for Biocatalysis: Modern Techniques and Applications*, edited by D. M. York and T.-S. Lee (Springer, New York, 2009), pp. 137–172.
[9] B. Jeziorski, R. Moszynski, and K. Szalewicz, Chem. Rev. (Washington, D.C.) **94**, 1887 (1994).
[10] A. J. Misquitta, R. Podeszwa, B. Jeziorski, and K. Szalewicz, J. Chem. Phys. **123**, 214103 (2005).
[11] K. Kitaura and K. Morokuma, Int. J. Quantum Chem. **10**, 325 (1976).
[12] T. Ziegler and A. Rauk, Theor. Chim. Acta **46**, 1 (1977).
[13] W. J. Stevens and W. H. Fink, Chem. Phys. Lett. **139**, 15 (1987).
[14] R. F. Frey and E. R. Davidson, J. Chem. Phys. **90**, 5555 (1989).
[15] P. S. Bagus and F. Illas, J. Chem. Phys. **96**, 8962 (1992).
[16] A. van der Vaart and K. M. Merz, Jr., J. Phys. Chem. A **103**, 3321 (1999).
[17] E. D. Glendening and A. Streitwieser, J. Chem. Phys. **100**, 2900 (1994).
[18] W. Chen and M. S. Gordon, J. Phys. Chem. **100**, 14316 (1996).
[19] Y. Mo, J. Gao, and S. D. Peyerimhoff, J. Chem. Phys. **112**, 5530 (2000).
[20] M. A. Blanco, A. M. Pendás, and E. Francisco, J. Chem. Theory Comput. **1**, 1096 (2005).
[21] I. Mayer, Phys. Chem. Chem. Phys. **8**, 4630 (2006).
[22] R. Z. Khaliullin, E. A. Cobar, R. C. Lochan, A. T. Bell, and M. Head-Gordon, J. Phys. Chem. A **111**, 8753 (2007).
[23] P. Reinhardt, J. P. Piquemal, and A. Savin, J. Chem. Theory Comput. **4**, 2020 (2008).
[24] M. P. Mitoraj, A. Michalak, and T. Ziegler, J. Chem. Theory Comput. **5**, 962 (2009).
[25] P. Su and H. Li, J. Chem. Phys. **131**, 014102 (2009).
[26] S. Liu, J. Chem. Phys. **126**, 244103 (2007).
[27] T. K. Ghanty, V. N. Staroverov, P. R. Koren, and E. R. Davidson, J. Am. Chem. Soc. **122**, 1210 (2000).
[28] S. M. Cybulski and C. E. Seversen, J. Chem. Phys. **119**, 12704 (2003).
[29] E. D. Glendening, J. Phys. Chem. A **109**, 11936 (2005).
[30] Y. Mo, L. Song, and Y. Lin, J. Phys. Chem. A **111**, 8291 (2007).
[31] Q. Wu and W. Yang, J. Chem. Phys. **118**, 2498 (2003).
[32] Q. Wu and T. Van Voorhis, Phys. Rev. A **72**, 024502 (2005).
[33] S. F. Boys and F. Bernardi, Mol. Phys. **19**, 553 (1970).
[34] W. Yang and Q. Wu, Phys. Rev. Lett. **89**, 143002 (2002).
[35] V. N. Staroverov, G. E. Scuseria, and E. R. Davidson, J. Chem. Phys. **124**, 141103 (2006).
[36] C. Kollmar and M. Filatov, J. Chem. Phys. **127**, 114104 (2007).
[37] A. Görling, A. Heßelmann, M. Jones, and M. Levy, J. Chem. Phys. **128**, 104104 (2008).
[38] A. Heßelmann and A. Görling, Chem. Phys. Lett. **455**, 110 (2008).
[39] A. Heßelmann, A. W. Götz, F. Della Sala, and A. Görling, J. Chem. Phys.

127, 054102 (2007).
[40] T. Heaton-Burgess, F. A. Bulat, and W. Yang, Phys. Rev. Lett. **98**, 256401 (2007).
[41] F. A. Bulat, T. Heaton-Burgess, A. J. Cohen, and W. Yang, J. Chem. Phys. **127**, 174101 (2007).
[42] T. Heaton-Burgess and W. Yang, J. Chem. Phys. **129**, 194102 (2008).
[43] Q. Wu and T. Van Voorhis, J. Chem. Theory Comput. **2**, 765 (2006).
[44] Q. Wu, C. L. Cheng, and T. Van Voorhis, J. Chem. Phys. **127**, 164119 (2007).
[45] A. D. Becke, J. Chem. Phys. **88**, 2547 (1988).
[46] Q. Wu and T. Van Voorhis, J. Chem. Phys. **125**, 164105 (2006).
[47] P. W. Ayers (unpublished).
[48] Y. Shao, L. Fusti-Molnar, Y. Jung, J. Kussmann, C. Ochsenfeld, S. T. Brown, A. T. B. Gilbert, L. V. Slipchenko, S. V. Levchenko, D. P. O'Neill, R. A. DiStasio, Jr., R. C. Lochan, T. Wang, G. J. O. Beran, N. A. Besley, J. M. Herbert, C. Y. Lin, T. Van Voorhis, S. H. Chien, A. Sodt, R. P. Steele, V. A. Rassolov, P. E. Maslen, P. P. Korambath, R. D. Adamson, B. Austin, J. Baker, E. F. C. Byrd, H. Dachsel, R. J. Doerksen, A. Dreuw, B. D. Dunietz, A. D. Dutoi, T. R. Furlani, S. R. Gwaltney, A. Heyden, S. Hirata, C.-P. Hsu, G. Kedziora, R. Z. Khalliulin, P. Klunzinger, A. M. Lee, M. S. Lee, W. Liang, I. Lotan, N. Nair, B. Peters, E. I. Proynov, P. A. Pieniazek, Y. M. Rhee, J. Ritchie, E. Rosta, C. D. Sherrill, A. C. Simmonett, J. E. Subotnik, H. Lee Woodcock III, W. Zhang, A. T. Bell, and A. K. Chakraborty, Phys. Chem. Chem. Phys. **8**, 3172 (2006).
[49] R. A. Kendall, E. Aprà, D. E. Bernholdt, E. J. Bylaska, M. Dupuis, G. I. Fann, R. J. Harrison, J. Ju, J. A. Nichols, J. Nieplocha, T. P. Straatsma, T. L. Windus, and A. T. Wong, Comput. Phys. Commun. **128**, 260 (2000).
[50] P. Barnes, J. L. Finney, J. D. Nicholas, and J. E. Quinn, Nature **282**, 459 (1979).
[51] P. Ren and J. W. Ponder, J. Phys. Chem. B **107**, 5933 (2003).
[52] E. D. Isaacs, A. Shukla, P. M. Platzman, D. R. Hamann, B. Barbiellini, and C. A. Tulk, Phys. Rev. Lett. **82**, 600 (1999).
[53] S. J. Chakravorty and E. R. Davidson, J. Phys. Chem. **97**, 6373 (1993).
[54] J. P. Piquemal, A. Marquez, O. Parisel, and C. Giessner-Prettre, J. Comput. Chem. **26**, 1052 (2005).
[55] M. Dreyfus, B. Maigret, and A. Pullman, Theor. Chim. Acta **17**, 109 (1970).
[56] M. Dreyfus and A. Pullman, Theor. Chim. Acta **19**, 20 (1970).
[57] J. Florian and B. G. Johnson, J. Phys. Chem. **99**, 5899 (1995).
[58] J. H. Lii and N. L. Allinger, J. Comput. Chem. **19**, 1001 (1998).
[59] J. Sponer and P. Hobza, J. Phys. Chem. A **104**, 4592 (2000).
[60] J. F. Beck and Y. Mo, J. Comput. Chem. **28**, 455 (2007).
[61] R. Vargas, J. Garza, R. A. Friesner, H. Stern, B. P. Hay, and D. A. Dixon, J. Phys. Chem. A **105**, 4963 (2001).
[62] E. M. Cabaleiro-Lago and J. R. Otero, J. Chem. Phys. **117**, 1621 (2002).
[63] A. V. Morozov, T. Kortemme, K. Tsemekhman, and D. Baker, Proc. Natl. Acad. Sci. U.S.A. **101**, 6946 (2004).
[64] Q. Wu and W. Yang, J. Chem. Phys. **116**, 515 (2002).
[65] S. Grimme, J. Comput. Chem. **25**, 1463 (2004).
[66] S. Grimme, J. Comput. Chem. **27**, 9095 (2006).
[67] M. Dion, H. Rydberg, E. Schröder, D. Langreth, and B. Lundqvist, Phys. Rev. Lett. **92**, 246401 (2004).
[68] T. Thonhauser, V. Cooper, S. Li, A. Puzder, P. Hyldgaard, and D. Langreth, Phys. Rev. B **76**, 125112 (2007).
[69] A. Becke and E. Johnson, J. Chem. Phys. **127**, 124108 (2007).
[70] O. Vydrov and T. Van Voorhis, J. Chem. Phys. **130**, 104105 (2009).